

Manuscript Number: CARBPOL-D-13-02768

Title: Solid state NMR and IR characterization of wood polymer structure in relation to tree provenance

Article Type: Research Paper

Keywords: solid state NMR spectroscopy, mid-infrared spectroscopy, wood provenance, PCA

Corresponding Author: Dr. jakub sandak, PhD

Corresponding Author's Institution: IVALSA/CNR

First Author: Ilaria Santoni, PhD

Order of Authors: Ilaria Santoni, PhD; Emanuela Callone, PhD; Anna Sandak, PhD; jakub sandak, PhD; Sandra Dirè Dirè, Prof.

Abstract: ¹³C nuclear magnetic resonance and mid-infrared spectroscopies were used for characterizing changes in the chemical structure of wood polymers (cellulose, hemicellulose and lignin) in relation to the tree growth location. Samples of three provenances in Europe (Finland, Poland and Italy) were selected for studies. The requirement was to use untreated solid wood samples to minimize any manipulation to the nanostructure of native wood. The measurement reliability of the NMR experiment has been quantified by means of internal reference in form of HDPE strip rolled together with wooden sample.

The results confirm that the chemical and physical properties of samples belonging to the same wood species (*Picea abies*) differ due to the origin. Both FT-IR and dynamic NMR spectroscopies were able to correctly discriminate samples originating from three different provenances in Europe. Such methods might be very useful for both, research and understanding of wood microstructure and its variability due to the growth conditions.

Suggested Reviewers: Roger Meder PhD
Group Leader, Tropical Production Forestry, CSIRO
Roger.Meder@csiro.au
expert in wood, NMR and chemometrics

Philippe Gerardin Prof.
Laboratory of Research and Wood Material, Lorraine University
philippe.gerardin@univ-lorraine.fr
an expert in wood, wood chemistry and chemical analysis

Carmen-Mihaela Popescu PhD
Petru Poni Institute of Macromolecular Chemistry, Romanian Academy
mihapop@icmpp.ro
an expert in wood, chemistry, NMR and chemometry

Dear Editor,

Please find attached our manuscript entitled “**Solid state NMR and IR characterization of wood polymer structure in relation to tree provenance**”, describing the results of both nuclear magnetic resonance and infrared spectroscopies studies on wood from different European areas. The wood of different geographical origins differs in term of chemical, phenological and physical properties (as mentioned in the Introduction of our manuscript). However, it is a very hard task to define/describe such differences. The development of a reliable technique allowing classification of wood in regard to its provenance is therefore of great interest.

The work here proposed is a continuation of our previous research, where NIR spectroscopy has been successfully applied for the differentiation of wood samples. The previous results were convincing, but there were several questions regarding the link between spectrum differentiation and polymer structures. The joint use of different techniques and skills has been an important step toward better understanding of the factors that discriminate among the wood samples, at the molecular level (related to protons mobility and chemical functional groups). To our knowledge no such research was reported before.

We do sincerely believe that the content and way of presentation of our manuscript would be of interest for the Carbohydrates Polymer readers. Thus, we are submitting our work as an original full-length research paper.

Looking forward to have your kind evaluation,
With sincerely regards,

Jakub Sandak, on behalf of authors

Highlights

- FT-IR and NMR spectroscopies were used for the discrimination of samples with different geographical provenance
- $T_{1\rho(H)}$ values, obtained from Variable Contact Time NMR experiments highlighted the differences between wood groups
- Principle Component Analysis of NMR and IR data allowed the most effective discrimination of wood due to provenance

1 **Solid state NMR and IR characterization of wood polymer structure in relation to tree**
2 **provenance**

3

4

5

6 **Ilaria Santoni,¹ Emanuela Callone,² Anna Sandak,¹ Jakub Sandak,¹✉ and Sandra Dirè²**

7

8

9 ¹ **Trees and Timber Institute IVALSA/CNR, via Biasi 75, 38010 San Michele All'Adige**
10 **(Italy)**

11 ² **Industrial Engineering Department, University of Trento, v. Mesiano 77, 38123 Trento**
12 **(Italy)**

13

14 santoni@ivalsa.cnr.it, callonee@ing.unitn.it, anna.sandak@ivalsa.cnr.it, sandak@ivalsa.cnr.it,
15 sandra.dire@ing.unitn.it

16

17 **corresponding author:** Jakub Sandak, Trees and Timber Institute IVALSA/CNR, via Biasi
18 75, 38010 San Michele All'Adige (Italy), ✉ sandak@ivalsa.cnr.it, tel: +390461660232, fax:
19 +390461650045

20

21

22

23 ***Abstract***

24

25 ¹³C nuclear magnetic resonance and mid-infrared spectroscopies were used for characterizing
26 changes in the chemical structure of wood polymers (cellulose, hemicellulose and lignin) in
27 relation to the tree growth location. Samples of three provenances in Europe (Finland, Poland
28 and Italy) were selected for studies. The requirement was to use untreated solid wood samples
29 to minimize any manipulation to the nanostructure of native wood. The measurement
30 reliability of the NMR experiment has been quantified by means of internal reference in form
31 of HDPE strip rolled together with wooden sample.

32 The results confirm that the chemical and physical properties of samples belonging to the
33 same wood species (*Picea abies*) differ due to the origin. Both FT-IR and dynamic NMR
34 spectroscopies were able to correctly discriminate samples originating from three different
35 provenances in Europe. Such methods might be very useful for both, research and
36 understanding of wood microstructure and its variability due to the growth conditions.

37

38

39 ***Highlights***

- 40 • FT-IR and NMR spectroscopies were used for the discrimination of samples with
41 different geographical provenance
- 42 • $T_{1\rho(H)}$ values, obtained from Variable Contact Time NMR experiments highlighted the
43 differences between wood groups
- 44 • Principle Component Analysis of NMR and IR data allowed the most effective
45 discrimination of wood due to provenance

46

47 ***Key words***

48 solid state NMR spectroscopy, mid-infrared spectroscopy, wood provenance, PCA

49

50

51



52 1. Introduction

53
54 The adaptation of species had been scientifically demonstrated by Charles Darwin already in
55 1868. Local climate, soil, slope, forest density, silvicultural practices, fungi, wildlife, disease
56 and other factors can strongly influence the tree growth and consequently, wood formation.
57 The timber in a given site carries a record of all the conditions listed above. As an adaptation
58 mechanism of trees to different site conditions several variations in the tree-ring structure
59 have been observed by Miina (2000), Park & Spicker (2005), Manetti & Cutini (2006) and
60 Andreassen, Solberg, Tveito & Lystad (2006) among others. Norway spruce (*Picea abies*),
61 often called whitewood, is a northern and central European species, living primarily in the
62 mountainous areas. The vertical limit for the spruce presence in the Alps is at an altitude of
63 ~2,200m. There are three main regions of spruce presence in Europe;

- 64 • Scandinavia, West Siberia (up to the Urals), Belarus and Northeast Poland
- 65 • mountainous areas of Central Europe – the Sudetes and the Carpathian Mountains
- 66 • Southern Europe including the Balkans and the Alps

67 According to recent forest inventories, the actual distribution of spruce is much wider than its
68 natural ranging (Spicker, 2000).

69
70 The Norway spruce wood from northern provenances (Scandinavian countries) has the
71 highest overall density and percentage of latewood comparing to trees growing in Central and
72 Southern Europe (Skrøppa, Hysten & Dietrichson, 1999). Krzysik (1978) reported that
73 different amounts of cellulose, hemicelluloses, lignin, and extractive components were
74 measured in spruce wood from different provenances. Analogous observations were noticed
75 for other wood species; *Eucalyptus globus* (Miranda & Pereira, 2002), *Pinus helepensis*
76 (Tahar, Tayeb & Chaabane, 2007), *Pinus ponderosa* (Smith, Peloquin & Passoff, 1969). It is
77 expected, therefore, that trees growing in various parts of the world would differ in such a
78 way to discriminate their specific distinctive features.

79
80 The currently employed PEFC (Programme for the Endorsement of Forest Certification), used
81 for tracking the wood flow from the forest to the mill system, is based only on written
82 documentation. Several methods including chemical and genetic fingerprinting are currently
83 employed for verification of product identity by examining its chemical or genetic
84 composition (Dykstra *et al.* 2002). Chemical fingerprinting methods include: analysis of trace
85 elements, pyrolysis, gas chromatography, as well as, near- and mid- infrared spectroscopies.
86 Genetic fingerprinting methods consist of DNA marker analysis from one or more of the
87 following genomes: nuclear, plastid or mitochondrial. Even if several successful applications
88 of the above techniques have already been reported, (Nielsen & Kjær, 2008, Sandak, Sandak
89 & Negri, 2010, 2011) none of these methodologies has reached a stage of development that
90 would warrant its general use up to this point. Some techniques are too costly and/or time
91 consuming for routinely use in timber tracking. These applications are limited to a small
92 number of samples, to be investigated in the laboratory. In contrary, infrared spectroscopy is a
93 fast and non-destructive method. Unfortunately, the detailed interpretation of spectra and the
94 following correlation of acquired data in order to discriminate the provenance are still
95 questionable. Therefore, an additional research supporting better understanding of the infrared
96 relation with wood provenance is of great interest.

97 Nuclear magnetic resonance (NMR) is becoming a routine technique in agro-food fields for
98 quality control and traceability of cheese and wine (Sacchi & Paolillo, 2007, Aghemo,
99 Albertino, & Gobetto, 2011, Mazzei & Piccolo, 2012, Ritota *et al.* 2012, Ritota, Casciani,
100 Failla, & Valentini, 2012). It is expected, therefore, that it might have also a great potential
101 for wood characterization. Several researchers have proposed the use of NMR for detailed
102 investigation of the chemical structure of wood (Gil & Neto, 1999, Maunu, 2002, Bardet *et al.*

103 2009, Mburu, Dumarçay, Huber, Petrissans, & Gerardin, 2007). Thus, many papers focus on
104 the structural differences between natural and treated wood-based materials, the efficiency of
105 chemical extraction methodologies, and characterization of its polymeric components. NMR
106 characterization of wood was a subject in the archaeological research to test the wood aging
107 and storage effects of historical materials (Bardet, Foray, & Tran, 2002, Bardet, Foray,
108 Maron, Goncalves, & Tran, 2004, Crestini, Hadidi, & Palleschi, 2009). It has also been used
109 for monitoring the decomposition level of forested areas (Preston, Trofymow, Niu & Fyfe,
110 1998).

111 Wood is, in its nature, a complex and heterogeneous material, considered as a matrix of three
112 main polymers: cellulose, hemicellulose and lignin. The advantage of NMR technique is,
113 therefore, in its ability to analyse a mixture of such polymers without extensive chemical
114 modifications to obtain separated fractions. Several authors have reported NMR research
115 results on lignin structures (Nimz, Robert, Faix, & Nemr, 1981, Malkavaara, Alén, &
116 Kolehmainen, 2000, Capanema, Balakshin & Kadla, 2004). Other studies have been dedicated
117 to woody carbohydrates, hemicelluloses (Gil & Neto, 1999, Maunu, 2002) and cellulose
118 (Newmann, 1999, Larsson, Hult, Wickholm, Pettersson, & Iversen, 1999, Okushita, Komatsu,
119 Chikayama, & Kikuchi, 2012). These have been a starting point for the following research on
120 wood by solid state NMR. This has dealt with the structural modifications induced directly by
121 processes such as pyrolysis, densification, bleaching, pulping or biodegradation (Sivonen,
122 Maunu, Sundholm, Jamsa, & Viitaniemi 2002, Delmotte, Ganne-Chédeville, Leban, Pizzi, &
123 Pichelin, 2008, Popescu, Larsson, & Vasile, 2011). Over the past 30 years, the technical
124 advances of NMR instrument hardware and the evolution of theoretical knowledge have made
125 it possible to vary sequences and to apply high magnetic fields and spinning speeds in order to
126 study wood, especially with ¹H, ¹³C and ³¹P magic angle spinning (MAS) NMR. Recently,
127 the ¹³C cross polarization magic angle spinning (CPMAS) is the most used NMR technique
128 for wood characterization, due to the high signal-to-noise ratio obtainable in a relatively short
129 experimental time, despite the loss of quantitative reliability. However, it must be noted here
130 that physical manipulation of wood, such as scratching and grinding while preparing suitable
131 samples lead to changes in its polymeric structure, i.e. the composition appears to be method
132 dependent to some extent (Viel, Capitani, Proietti, Ziarelli, & Segre, 2004, Bardet, Foray, &
133 Tran, 2002). This means that the results of liquid and solid state NMR analyses of isolated
134 components are not comparable and, therefore, provide little information on the original
135 structure of solid wood. Small cylindrical samples were thus proposed to get a fingerprint of
136 the pristine material (Preston, Trofymow, Niu, & Fyfe, 1998, Bardet *et al.* 2009). The
137 preparation process of such samples made of wood is rather complicated. Therefore, an
138 alternative procedure should assure a proper representation of the complex wood structure
139 while minimizing any chemo-physical manipulation of the wood during sample preparation.

140
141 Taking into account the above considerations, the aim of this research was to develop an
142 original MAS NMR-based methodology (including experimental set-up and wooden sample
143 preparation) for studies of chemical/physical wood properties.. The overall objective was to
144 characterize cellulose, hemicellulose and lignin of selected wood samples possessing intra-
145 species differences resulting from variation of geographical provenance. Both IR and NMR
146 spectroscopies, assisted by modern multivariate analysis, were investigated.

147
148
149
150
151
152
153



154 **2. Material and methods**

155

156 **2.1. Material selection**

157 Sets of Norway spruce (*Picea abies* L. Karst.) wood samples collected in three different
158 locations within Europe were used as experimental materials. The countries of origin included
159 Finland, Poland and Italy, all differing in geographical position, elevation, climate and
160 silviculture. The summary of site characteristics is presented in Table 1. The procedure of
161 samples harvesting, conditioning and preparation was described previously (Sandak, Sandak,
162 & Negri, 2011). Because it was impossible to collect trees of exactly the same age,
163 experimental samples were obtained from the adult wood zones assuring equal cambial age of
164 the all investigated samples.

165

166

167 **Table 1. General characteristics of the provenance sites**

168

169

170 **2.2. Chemical composition**

171 The chemical content of main woody polymers was determined on milled samples from each
172 provenance.

173 The concentration of cellulose was determined according to the Seifert procedure (by using
174 acetylacetone-dioxane-hydrochloric acid). Holocellulose content was obtained by wood
175 delignification with sodium chlorite with the addition of acetic acid (Browning, 1967). The
176 content of hemicellulose was computed as the difference between holocellulose and cellulose.
177 The quantities of other wood components were determined according to the following
178 standards:

179 lignin (TAPPI T 222 om-06)

180 hot water extractives (TAPPI T 207 cm-08)

181 1% NaOH extractives (TAPPI T 212 om-07)

182 organic solvent extractives (TAPPI T 204 cm-07)

183 ash content (TAPPI T 211 om-07)

184 The chemical analyses were repeated three times and maximum standard deviation of results
185 was considered as a measurement error indicator.

186

187 **2.3. FT-IR-ATR analysis**

188 The set of 30 samples (10 for each provenance) were analyzed by means of mid infrared
189 spectroscopy using an FT-IR spectrometer (ALPHA produced by Bruker Optics GmbH)
190 equipped with a ZnSe external module for attenuated total reflection (ATR) with the
191 following settings: 24 scans per sample; spectral resolution: 4cm⁻¹, wavenumber range: 4000
192 to 600 cm⁻¹. The OPUS 7.0 (by Bruker Optics) software package was used for instrument
193 control and data processing. An original procedure for selection of the representative samples
194 was established on the base of samples homogeneity. Firstly, an average spectrum
195 representing one provenance was calculated from the set of all spectra acquired within
196 samples of same provenance. Three samples with spectra closest (in term of spectral distance)
197 to the average value were selected for NMR analysis. The homogeneity was quantified on the
198 base of cluster analysis. The selection was essential to diminish the natural variability of
199 woody material and to assure a compromise between the generality of results and the
200 relatively time consuming NMR analyses.

201

202 **2.4. NMR analysis**

203 The Nuclear Magnetic Resonance measurements were restricted to the nine representative
204 samples (P1-P3, I1-I3, F1-F3) selected from the set 30 samples measured by FT-IR. MAS
205 NMR analyses were carried out with a Bruker 300WB instrument operating at a proton

206 frequency of 300.13 MHz. NMR spectra were acquired with a cross-polarization (CP) pulse
207 sequence under the following conditions: ^{13}C frequency: 100.07 MHz, $\pi/2$ pulse length: 3.5
208 μs , ^1H decoupling pulse power: 47 kHz, recycle delay: 3 s, contact time range: 0.2 – 9 ms, 2k
209 scans. Samples in the form of rolled thin wood slices were packed in 4mm diameter zirconia
210 rotors, which were spun at 8 kHz under air flow. Both the sample shape and size ensure the
211 use of a representative sample.

212 In addition, the use of an internal standard was evaluated in order to ensure quantitative
213 analysis and to estimate the measurement stability. For this purpose, a high density
214 polyethylene (HDPE) film, with a mass of about 10% the corresponding wood weight, was
215 rolled together with the wooden slice. The HDPE did not affected the NMR spectrum, its
216 peak does not overlap with the wood signals. Bruker Topspin 1.3 software was used for data
217 analysis and spectra deconvolution.

218 Basic CPMAS experiments were recorded to identify the main signals assigned to the wood
219 and the HDPE. Since intrinsic parameters, like conformation and mobility depend both on
220 homonuclear and heteronuclear interactions, variable contact time experiments (VCT) were
221 performed in order to obtain complementary information. The CP spectrum intensity depends
222 on two competing factors, the magnetization transfer by dipolar coupling and the spin-lattice
223 relaxation times in the rotating frame. Thus, measuring spectrum intensity (M) as a function
224 of CP contact time (t), it is possible to extract cross-relaxation parameters T_{CH} (cross-
225 polarization rate constant) and $T_{1\rho(H)}$ (spin-lattice relaxation time) (Equation 1). Numerical
226 estimation of T_{CH} and $T_{1\rho(H)}$ values are usually obtained by fitting the obtained experimental
227 curve with single or multiple exponential laws according to homogeneity, segregation and/or
228 domain size (Kolodziejcki & Klinowski, 2002).

$$230 \quad M(t) = M_0 \cdot e^{\frac{-t}{T_{1\rho(H)}}} \cdot (1 - e^{\frac{-t}{T_{CH}}}) \quad \text{equation 1}$$

231
232 where; $M(t)$ is the peak intensity as a function of contact time t , M_0 is the normalization
233 constant, $T_{1\rho(H)}$ is the proton spin-lattice relaxation time in the rotating frame, and T_{CH} is the
234 cross-polarization time constant.

236 2.5. Multivariate data analysis

237 Principal Component Analysis (PCA) and Cluster Analysis (CA) were used for evaluation of
238 spectral data obtained by FT-IR and NMR spectroscopies. Mid infrared spectra were post-
239 processed and evaluated with OPUS 7.0 software (Bruker Optics GmbH). Ward's algorithm
240 and the calculation of Euclidean distances was applied when creating dendrograms of the CA.
241 Identity test (part of the Opus package) was used for development of the PCA models
242 discriminating woods due to the provenance. Unscrambler 10.2 (Camo Software) was used
243 for PCA analysis of NMR data.

244

245

246

247

248 3. Results and Discussions

249

250 The chemical composition of Norway spruce samples representing three different
251 provenances is presented in Table 2. The apparent difference between quantities of cellulose
252 and holocellulose within samples of all locations are negligible and smaller than the
253 measurement error. It was not possible, however, to explain (by wet chemistry analysis) the
254 possible qualitative differences between carbohydrates extracted from woods of different

255 origin. Some more evident differentiation was, however, noticeable for the lignin and
256 extractives content.

257
258

259 ***Table 2. Contents of chemical components extracted from Norway spruce samples of***
260 ***different provenances***

261
262 Selected physical properties, as summarized in Table 3, indicate clear morphological
263 differentiation of spruce samples from Finland, Poland and Italy. The specific density and the
264 late wood ratio of Italian wood samples were the lowest. The highest ring width was noticed
265 for wood from Poland. The tendency followed the results of Franceschini et al. (2010) where
266 the ring width is negatively correlated with the tree age. The yearly ring size was comparable
267 for samples from Finland and Italy, even if the geographical locations were the most distant.
268 However, the climatic conditions, especially the average yearly temperature and the length of
269 vegetation season, were similar in both Finland and Italy.

270
271

272 ***Table 3. Physical characteristic of spruce samples.***

273
274

275 Figure 1 presents results of FT-IR Principle Components Analysis (PCA) performed on
276 spectra collected from wood samples of three different provenances. A clear separation
277 between groups was achieved after plotting the three first PC scores on the graph. These
278 results for mid-IR are in correspondence with previous studies using near-IR. They proved
279 that wood of the same species (*Picea abies*) from different provenance can be separated
280 through FT-NIR spectroscopy (Sandak; Sandak, & Negri, 2011). The question rises here:
281 what are the chemical/physical bases for such distinction of different spruce woods.

282
283

284 ***Figure 1. FT-IR-based discrimination of the spruce woods due to provenance***

285
286

287 It is clear that the infrared spectroscopy, due to its functioning principle, is only capable of
288 detecting the presence of functional groups such as -OH, -CH or -CH₂. The three structural
289 polymers (cellulose, hemicelluloses and lignin) have an extremely complex cross-
290 configuration and make up 90 – 98% of the woody matter. This makes IR spectroscopy
291 insufficient to fully characterize wood at the molecular level. The chemical structure of
292 cellulose, hemicelluloses and lignin is schematically presented in Figure 2.

293
294

295 ***Figure 2. The chemical structures of the main wood components (according to Bardet et al.***
296 ***2009): cellulose (a), hemicellulose (b) and lignin (c), and the numbering scheme***
297 ***corresponding to the resonance peaks summarized in Table 4***

298
299

300 Cellulose is present in wood as microfibrils and as amorphous regions. The microfibril
301 structure is crystalline and characterized by a high degree of polymerization. The quantity and
302 quality of the amorphous regions of cellulose differ due to species and the growing conditions
303 of the tree. The chemical structure of lignin is very complex and it is, in fact, impossible to
304 determine its precise composition as it varies even between trees in the same forest. In
305 softwoods, it is an amorphous polymer consisting of p-hydroxyphenyl -guaiacyl units (p-
306 hydroxyphenyl -syringil-guaiacyl in case of hardwoods) inter-linked in non-regular structures.

307 Lignin is hydrophobic, where cellulose is highly hydrophilic. Hemicellulose connects lignin
308 and cellulose together. Beside of genetic factors; the growing environment (including climate,
309 soil, silviculture and the yearly variation of sun/rain), strongly affects wood physiology,
310 xylogenesis, tree morphology and, in consequence, wood chemical composition.

311
312 FT-IR spectroscopy, through detection of the main functional groups, ensures a good
313 separation among wood samples, but cannot give an overall picture of the materials.
314 Therefore, solid state NMR was selected as an additional technique for providing
315 supplementary/alternative set of information on the molecular structure at short and medium
316 order.

317 As already mentioned, a good fingerprint of wood samples can be obtained with ¹³C CPMAS
318 NMR measurements. Representative NMR spectra of wood from Finland, Poland and Italy
319 are shown in Figure 3. The spectra present the typical resonances of wood components that
320 produce highly overlapped signals. Two key regions; from 160 to 110 ppm and from 110 to
321 15 ppm, can be distinguished in the NMR spectra, according to Bardet et al. (2009). The first
322 is characterized by broad and low intensity resonances typical of the aromatic structures in
323 lignin. The second region includes sharp intense peaks due to carbohydrate polymers
324 (cellulose and hemicellulose) that are highly overlapping each other due to their chemical
325 similarity.

326 Table 4 shows the resonance assignments (indicated by the numbering scheme in Figure 3 and
327 corresponding to the carbon atoms labeled in Figure 2), It should be mentioned that ¹³C
328 CPMAS NMR spectroscopy allows for the distinction of chemically equivalent carbons in
329 different chain packings or conformation, as it is in the case of amorphous and crystalline
330 cellulose. The most intense peaks **11** and **12** are due to C-2, C-3 and C-5 carbons in glucose.
331 The two peaks **9** and **10** are assigned to C-4, in crystalline and amorphous (or less ordered
332 surface) cellulose, respectively. Peak **14** is related to C-6 in cellulose and C_γ in lignin. Peak **8**
333 represents cellulose's C-1 with a high-field shoulder attributed to hemicellulose (103 ppm).
334 Only two signals can be undoubtedly attributed to hemicellulose: the methyl carbon peak **17**
335 and the carboxylic carbon signal **1**, although these are of rather weak intensity. The three
336 aromatic units constituting the lignin lattice are recognized from three groups of signals in the
337 range 160-105 ppm. Finally, the small peak **15** is assigned to the lignin methoxyl group.

338
339

340 *Figure 3 NMR spectra of spruce woods differing in provenance and the peaks assignments*

341
342

343 *Table 4. ¹³C CPMAS resonance assignments of wood and HDPE*

344
345

346 The three representative NMR spectra of Figure 3 suggest that all the provenances (P, F and I)
347 produce similar signals and only minor intensity differences can be noticed without a
348 quantitative analysis, for example: lignin's peaks (**3**, **6**, **7**, **14**) and carbohydrates' signals (**1**,
349 **13**, **17**).

350 Chemically equivalent carbons produce the same response to cross-polarization and the
351 resulting peak areas are comparable. For that reason, an internal standard has been used
352 allowing for both quantitative spectra evaluation and probing the stability of the dynamic
353 NMR measurements. The polyethylene standard produces a sharp peak at 32 ppm
354 corresponding to the methylene carbon of the polymer backbone (**16** in Figure 3). The peak
355 does not overlap with wood signals and, in consequence, its intensity may be used for signal
356 normalization and the estimation of the measurement error.

357

358 It has been reported (Teeäär, Serimaa, & Paakkarl, 1987 and Mansfield, & Meder, 2003) that
359 the cellulose crystalline index CrI can be calculated on the basis of NMR spectra according to
360 equation 2.
361

$$362 \quad CrI = \frac{A_9}{A_9 + A_{10}} \quad \text{equation 2}$$

363 where: A_9 and A_{10} are the de-convoluted peak areas of signals **9** and **10** corresponding to the
364 C-4 carbon atom.
365

366 The range of CrI values were computed for the investigated samples, as shown in Figure 4,
367 and correspond to the reference literature data (Samuel, Pu, Faston, & Ragaukas, 2010, Park,
368 2010). It can be noticed that spruce samples originating from Poland have higher CrI than the
369 other two series. Even if there is a clear trend, it has to be mentioned that nominal differences
370 are too small to draw any conclusion.
371

372
373 **Figure 4. Cellulose crystalline index CrI computed from the NMR spectra of spruce from**
374 **different provenance**
375
376

377 Additional NMR analyses were done because the straightforward comparison of raw NMR
378 spectra was not sufficient for undoubtable discrimination of the wood provenances. Dynamic
379 NMR measurements were, therefore, performed in order to provide supplementary
380 information on the polymeric interconnections testing wider material domains. A series of
381 CPMAS spectra were collected for each sample varying the contact time (ct) between 0.2 and
382 9.0 ms. The calculated signal intensity vs. contact time was compared after the normalization
383 of the peak height. To neglect differences due to variations in sample weights, the intensity
384 values of the selected peak y_n were extracted from the spectra and normalized with respect to
385 the corresponding peak intensity at $ct=1$ ms (y_1) according to Equation 3:
386

$$387 \quad y'_n = \frac{y_n}{y_1} \cdot 100 \quad \text{equation 3}$$

388
389 The resulting y'_n values were then plotted against the contact time. The HDPE signal (**16**) was
390 used to ensure the reproducibility of the measurement procedure. The obtained results are
391 presented in Figure 5a. The HDPE VCT curves show similar profiles independently of the
392 wood sample. The reproducibility of the measurements was good except for the shortest and
393 the longest contact times, due to the relatively low peak intensity. Thus for the peak **16**, the
394 calculated measurement percentage error was $\pm 6\%$.
395

396 Since CP spectral intensity is a measure of the efficiency of magnetization transfer from 1H to
397 ^{13}C by the dipolar coupling, the CP time constant (T_{CH}) can give a quantitative description of
398 the cross-polarization and relaxation behaviour (Abelmann, Totsche, Knicker, & Kogel-
399 Knabner, 2004, Cheng, Wartelle, & Klasson, 2010). The less mobile carbon groups exhibit
400 both fast cross-polarization rate, i.e. short T_{CH} , because the cross-polarization is most efficient
401 for the static 1H - ^{13}C dipolar interactions, and long $T_{1\rho(H)}$ values. As mobility increases (i.e.,
402 with increasing amorphous or homogeneous character of sample series) T_{CH} increases and
403 $T_{1\rho(H)}$ decreases. It has been demonstrated that the measure of $T_{1\rho(H)}$ relaxation time can be
404 used to estimate the domain size in polymers. (Conte, Spaccini, & Piccolo, 2006). Diffusion
405 of 1H magnetization within a hybrid system tends to average the 1H relaxation time thus

406 leading to an averaging effect on the $T_{1\rho(H)}$ of the different components. In a homogeneous
407 system, a single spin-lattice relaxation time is usually observed. For a heterogeneous system,
408 more than one $T_{1\rho(H)}$ value are often found, because there is insufficient time for spin diffusion
409 to equilibrate the magnetization in different phases (Kao, Chao, & Chang, 2006). Through
410 measures of contact time variation, mobility and interactions of polymers can be studied
411 (Bardet *et al.* 2009, Okushita, Komatsu, Chikayama, & Kikuchi, 2012). As a matter of fact,
412 similar relaxation times of polymeric species inside the same matrix correspond to chemical
413 interactions between chains (Liitia, Maunu, & Hortling, 2000, 2001, Bardet *et al.* 2009).

414
415
416 **Figure 5. Normalized peak intensity vs ct of HDPE signal 16 (a) and wood signal 8 (b).**

417
418
419 HDPE is a homogeneous polymer, and therefore, the magnetization behaviour follows the
420 single exponential law (Equation 1). The calculated values of the two time constants were T_{CH}
421 = 0.17 μ s and $T_{1\rho(H)}$ = 21.1 μ s, in agreement with the results reported for HDPE measurements
422 in similar conditions (Nogueira, Tavares, Nogueira, 2004). It was possible to conclude
423 therefore that polyethylene was a suitable reference and that all the experimental results from
424 tests are comparable.

425
426 The wood spectra display intense sharp peaks together with weak and broad resonances. In
427 order to keep the confidence level of 6%, the exponential trend of intensity vs. contact time
428 was studied only for some selected peaks. These are the sharpest and fall in the range between
429 110 to 60 ppm. Accordingly, seven peaks were chosen: 8 C-1 from cellulose, 9 C-4 from
430 crystalline cellulose, 10 C-4 from amorphous cellulose and C β from lignin, 11 C2,3,5 from
431 cellulose and C α from lignin, 12 C2,3,5 from cellulose, 13 CH₂OH C-6, and 14 C γ from
432 lignin. Examples of the VCT curves related to peak 8 at 105ppm are presented in Figure 5b.
433 The above peak selection includes mainly the cellulose peaks, but the overall signal
434 overlapping ensures also the contribution of other woody polymers. Assuming that all the
435 carbons are in similar motional domains, the rising part of the exponential curve is dominated
436 by the static dipolar interaction between carbon atom and nearest neighbor protons (¹³C-1H
437 distance) described by the T_{CH} relaxation time. The T_{CH} values for the evaluated signals are
438 shown in Figure 6. It is clear that variations of T_{CH} do not display particular trends due to
439 sample provenance and any differences among the samples are not systematic.

440
441
442 **Figure 6. TCH values obtained from the fitting of VCT curves of selected ¹³C signals with**
443 **Equation 1.**

444
445
446 The obtained average T_{CH} values, around 0.7ms, can be considered as the result of the
447 presence of both rapidly and slowly cross-polarizing components, with a predominance of the
448 latter. In literature it was reported that the determination of T_{CH} is inherently difficult because,
449 in principle, there are as many T_{CH} values as there are chemical environments. In the studied
450 case, the values were closer to those typical of aromatics, in particular for samples from Italy
451 and Poland (Conte, Spaccini, & Piccolo, 2006). This could also be explained with the
452 presence of small proton-rich hydrophobic domains or short polymeric chains randomly
453 distributed within the wood cell walls.

454
455 In case of rigid and heterogeneous materials, such as wood, equation 1 is a good model
456 because the assumption $T_{CH} \ll T_{1\rho(H)}$ is satisfied. The effect of relaxation due to spin diffusion

457 is therefore commonly investigated (Smernik, Baldock, & Oades, 2002, Nogueira, Tavares, &
458 Nogueira, 2004). The $M(t)$ curve fitting was performed by means of only one exponential
459 factor, due to the high complexity of the system. Additionally, consideration of multiple
460 exponential fitting factors did not significantly improve the result. The average extrapolated
461 parameters $T_{1\rho(H)}$ for each peak are presented in Figure 7. It should be noticed that for most
462 peaks the $T_{1\rho(H)}$ values can be clustered according to the geographical provenance of wood. In
463 particular, samples from Finland, show uniform values that are clearly lower than those of
464 samples from other series. High values of $T_{1\rho(H)}$ are related to slow motion and minimised
465 variations among $T_{1\rho(H)}$ values for different peaks suggest an intimate connection among the
466 structural components of wood. Quite homogeneous values are found for the sample from
467 Poland, with the exception of peaks 10 and 12. The series of Italian woods posses more
468 scattered values, especially for peaks 8, 9, and 10. In general, samples from Italy and Poland
469 show rather analogous results with the exception of the resonance 8. The C-1 $T_{1\rho(H)}$ (peak 8)
470 produces the highest discrimination among samples and suggests that mobility increases
471 according to Italy<Poland<Finland trend.

472
473
474

475 **Figure 7. $T_{1\rho(H)}$ values obtained from fitting VCT curves of selected ^{13}C signals with Eq. 1**

476
477

478 As $T_{1\rho(H)}$ is derived from the molecular organization of polymers, it could be related to
479 some physical features of wood presented in Table 3. The trend of $T_{1\rho(H)}$ of the peak 8
480 (cellulose C-1) appeared to be inversely related to the sample density ($r^2=0.92$), implying that
481 smaller relaxation times correspond to higher density. Similarly, the $T_{1\rho(H)}$ of peak 9
482 (crystalline cellulose) can be linked to the quantity of latewood ($r^2=0.85$), i.e. samples with
483 higher latewood ratio show shorter relaxation time.

484 The peculiar characteristics of wood from Finland might be interpreted by distinct chemical
485 and physical properties of trees growing in Scandinavia, i.e. the highest wood density, high
486 ratio of late wood, and the high extractives content. All these are clearly related to the climatic
487 conditions that shorten the growth periods and stimulate the development of efficient defence
488 systems against local pathogens.

489
490

491 Multivariate analyses, similar to those performed on the FT-IR spectra were applied as well to
492 NMR data. The results obtained are summarized in Figure 8. The PCA discrimination of the
493 NMR spectra (obtained with $ct=1.0$ ms) did not provide sufficient differences for undoubtable
494 discrimination of wood samples from different provenances. As shown in Figure 8a, the
495 values of the samples from Poland (P1 and P3) overlapped the values of samples from Italy
496 (I3). Some improvement of the discrimination algorithm was achieved by computing the
497 principal components from VCT curves of selected peaks (8, 9, 11, 12, 13, 14) and is
498 presented in Figure 8b. Component PC1 alone (explaining 55% of the variance) was sufficient
499 for separation of Finnish samples from other provenances. On the other hand, the clear
500 discrimination of Polish samples from Italian samples on the basis of component PC3 was
501 limited as both clusters were close to each other and even slightly overlapping.

502
503

504 A significant improvement of the origin determination capability of the software was
505 achieved after performing PC analysis of the VCT experimental results, but only analysing
506 $T_{1\rho(H)}$ coefficients. As a matter of fact, it was impossible to create any reliable PCA model for
507 discrimination of wood origin based only on the T_{CH} coefficients. Figure 8c shows the
overlapping of the clusters even if both principal components covered over 83% of the

508 variance. This is in agreement with the previous considerations on T_{CH} presented in the NMR
509 section. The PCA scores from analysis of the $T_{I\rho(H)}$ coefficients are shown in Figure 8d. PC1
510 (explaining 81% of the variance within spectra) separates samples into two groups: Finland
511 (with PC1 values of negative order) and Poland/Italy (with positive values of PC1).
512 Moreover, PC2 (explaining 12% of the data variance) separates samples coming from Italy
513 and those originating from Poland. The cluster distribution is slightly similar to that of Figure
514 8b, but the most important difference is the higher spectral distance of Italian and Polish
515 samples assuring an apparent differentiation of the wood provenance.

516
517
518 **Figure 8. Principal Components Analysis of; all NMR spectra (a), dataset of all the VCT**
519 **curves of selected peaks (b) and T_{CH} (c) and $T_{I\rho(H)}$ (d) computed from VCT curves**
520

521 522 523 524 **4. Conclusions**

525
526 The work presented here was devoted to the development of a novel methodology for
527 characterization and discrimination of a wood in regard to its origin on the basis of infrared
528 and nuclear magnetic resonance spectra. The requirement was to use untreated solid wood
529 samples to minimize any manipulation to the nanostructure of native wood. The results
530 confirm that the chemical and physical properties of samples belonging to the same wood
531 species (*Picea abies*) differ due to the origin. Both FT-IR and dynamic NMR spectroscopies
532 were able to correctly discriminate samples originating from three different provenances in
533 Europe. The successful discrimination by means of infrared spectroscopy was mostly related
534 to differences in the molecular configuration of the cellulose, hemicellulose and lignin
535 (related to functional groups as -OH, -CH and -CH₂). Although the number of analysed
536 samples in the present work cannot be considered statistically meaningful, the results clearly
537 indicated that FTIR outcomes can be confirmed by means of solid state nuclear magnetic
538 resonance. NMR, also permits to highlight additional differences both in the connections
539 among constitutional polymers and in the homogeneity of molecular domains within wood
540 samples of different provenances. The measurement reliability of the NMR experiment has
541 been quantified by means of internal reference in form of HDPE strip rolled together with
542 wooden sample. It was also possible to normalize the spectra according to the wood/HDPE
543 mass ratio.

544
545 The most effective chemometric tool for discrimination of spectra due to provenance was
546 principal components analysis. It provided reliable prediction models for infrared
547 spectroscopy, but was also very useful for analysis of NMR spectra. In the second case the
548 analysis of $T_{I\rho(H)}$ coefficients as computed from fitting the $M(t)$ curve was the most efficient.
549 Further interpretation of $T_{I\rho(H)}$ suggests a higher polymer mobility and a higher homogeneity
550 in wood from Finland. On the other hand, equally less homogeneity was noticed in wood
551 samples from both Italy and Poland. The highest crystalline index CrI was detected in Polish
552 samples. Discrimination of provenance was achieved by means of $T_{I\rho(H)}$ PC analyses. It was
553 expected, and followed both theoretical background and literature references.

554
555 Concluding, it was possible to apply presented methodologies for the characterization of
556 wood according to its origin by means of both infrared and nuclear magnetic resonance
557 spectroscopies. Such methods might be very useful for both, research and understanding of
558 wood microstructure and its variations induced by growth conditions.

559
560
561
562
563
564
565
566
567
568
569
570
571
572
573
574
575
576
577
578
579
580
581
582
583
584
585
586
587
588
589
590
591
592
593
594
595
596
597
598
599
600
601
602
603
604
605
606
607
608

Acknowledgments

Part of this work has been conducted within the framework of the project SWORFISH (team 2009 incoming (CALL 2) and Trentino—PCOFUND-GA-2008-226070) co-financed by Provincia Autonoma di Trento. John Downs, PhD, is greatly acknowledged for the English text revision.

References

- Abelmann, K., Totsche, K.U., Knicker, H., & Kogel-Knabner, I. (2004) CP dynamics of heterogeneous organic material: characterization of molecular domains in coal. *Solid State Nucl Magn Reson.* 25, 252-266.
- Aghemo, C., Albertino, A., & Gobetto, R. (2011) Isotopic Analysis and ¹H-NMR Spectroscopy for Traceability and Discrimination of Italian Wines. In: J.P Renou, G.A. Webb, & P.S. Belton (Eds.), *Magnetic Resonance in Food Science: An Exciting Future* (pp. 30-35) Cambridge: RCS Publications.
- Andreassen, K., Solberg, S., Tveito, O.E., & Lystad, S.L. (2006) Regional differences in climatic responses of Norway spruce (*Picea abies* L. Karst) growth in Norway. *Forest Ecology & Management* 222, 211–221.
- Bardet, M., Foray, M.F., Maron, S., Goncalves, P., & Tran, Q.K (2004) Characterization of wood components of Portuguese medieval dugout canoes with high-resolution solid-state NMR. *Carbohydrate Polymers* 57, 419–424.
- Bardet, M., Foray, M.F., & Tran, Q.K. (2002) High-Resolution Solid-State CPMAS NMR Study of Archaeological Woods. *Anal. Chem.* 74, 4386-4390.
- Bardet, M., Gerbaud, G., Giffard, M., Doan, C., Hediger, S., & Le Pape, L. (2009) ¹³C high resolution solid-state NMR for structural elucidation of archaeological woods. *Prog Nucl Magn Res Spectrosc.* 55, 199–214.
- Browning, B.L. (1967) *The Chemistry of Wood.*, New York: Interscience (Wiley).
- Capanema, E.A., Balakshin, M.Y., & Kadla, J.F. (2004) A comprehensive approach for quantitative lignin characterization by NMR spectroscopy. *J Agric Food Chem.* 52, 1850–1860.
- Conte, P., Spaccini, R., & Piccolo, A. (2006) Advanced CPMAS-¹³C NMR techniques for molecular characterization of size-separated fractions from a soil humic acid. *Anal. Bioanal. Chem.* 386, 382-390.
- Cheng H.N., Wartelle L.H., Klasson K. T., & Edwards J.C. (2010) Solid-state NMR and ESR studies of activated carbons produced from pecan shells. *Carbon* 48, 2455– 2469.

609 Crestini, C., El Hadidi, N., & Palleschi, G. (2009) Characterization of archaeological wood: A
610 case study on the deterioration of a coffin. *Microchemical Journal* 92(2), 150-154.
611
612 Darwin, C. (1868) *The variation of animals and plants under domestication*. London: Murray,
613 (vol. 1).
614
615 Delmotte, L., Ganne-Chédeville, C., Leban, J.M., Pizzi, A. & Pichelin F. (2008) CP MAS
616 ¹³C NMR and FTIR investigation of the degradation reactions of polymer constituents in
617 wood welding. *Polymer Degradation and Stability* 93, 406-412.
618
619 Dykstra, D.P., Kuru, G., Taylor, R., Nussbaum, R. Magrath, W.B., & Story, J. (2002)
620 Technologies for Wood Tracking – Verifying and Monitoring the Chain of Custody and Legal
621 Compliance in the Timber Industry. Environment and Social Development East Asia and
622 Pacific Region Discussion Paper. World Bank – WWF Alliance report.
623 <http://www.proforest.net/publication> (accessed 30.10.2013)
624
625 Franceschini, T., Bontemps, J.D., Gelhaye, P., Rittie, D., Herve, J.C., Gegout, J.C., & Leban,
626 J.M. (2010) Decreasing trend and fluctuations in the mean ring density of Norway spruce
627 through the twentieth century. *Ann. For. Sci.* 67, 816.
628
629 Gil, A.M., & Neto, P.C. (1999) Solid state NMR studies of wood and other lignocellulosic
630 materials. *Annual Rep. NMR Spectrosc.* 37, 75–117.
631
632 Kao, H.M., Chao, S.W., & Chang, P.C. (2006) Multinuclear Solid-State NMR, Self-Diffusion
633 Coefficients, Differential Scanning Calorimetry, and Ionic Conductivity of Solid Organic-
634 Inorganic Hybrid Electrolytes Based on PPG-PEG-PPG, Diamine, Siloxane, and Lithium
635 Perchlorate. *Macromolecules* 39, 1029-1040.
636
637 Kolodziejski, W., & Klinowski, J. (2002) Kinetics of cross-polarization in solid state NMR: a
638 guide for chemists. *Chem. Rev.* 102, 613-628.
639
640 Krzysik, F. (1978) *Nauka o drewnie*. Warszawa:PWN (in Polish).
641
642 Larsson, P.T., Hult, E.L., Wickholm, K., Pettersson, E., & Iversen, T. (1999) CP/MAS ¹³C-
643 NMR spectroscopy applied to structure and interaction studies on cellulose I. *Sol. State*
644 *Nuclear Magn. Reson.* 15, 31–40.
645
646 Liitiä, T., Maunu, S.L., & Hortling, B. (2000) Solid state NMR studies on cellulose
647 crystallinity in fines and bulk fibers separated from refined kraft pulp. *Holzforschung* 54,
648 618–624.
649
650 Liitiä, T., Maunu, S.L., & Hortling, B. (2001) Solid state NMR studies on inhomogeneous
651 structure of fiber wall in kraft pulp. *Holzforschung* 55, 503–510.
652
653 Malkavaara, P., Alén, R., & Kolehmainen, E. (2000) Chemometrics: an important tool for the
654 modern chemist, an example from wood-processing chemistry. *J. Chem. Inf. Comput. Sci.* 40,
655 438–441.
656
657 Manetti, M.C., & Cutini, A. (2006) Tree-ring growth of Silver fir (*Abies alba* Mill.) in two
658 stands under different silvicultural systems in central Italy. *Dendrochronologia* 23:145–150.
659

660 Mannu, S.L. (2002) NMR studies of wood and wood products. *Progr. Nucl. Magn. Reson.*
661 *Spectrosc.* 40, 151–174.
662

663 Mansfield, S.D., & Meder, R. (2003) Cellulose hydrolysis – the role of monocomponent
664 cellulases in crystalline cellulose degradation. *Cellulose* 10, 159–169.
665

666 Mazzei, P., & Piccolo, A. (2012) ¹H HRMAS-NMR metabolomic to assess quality and
667 traceability of mozzarella cheese from Campania buffalo milk. *Food Chemistry* 132, 1620–
668 1627.
669

670 Mburu, F. Dumarcay, S. Huber, F., Petrissans, M. Gerardin, P. (2007) Evaluation of thermally
671 modified *Grevillea robusta* heartwood as an alternative to shortage of wood resource in
672 Kenya: Characterisation of physicochemical properties and improvement of bio-resistance.
673 *Bioresource Technology* 98, 3478–3486.
674

675 Miina, J. (2000) Dependence of tree-ring, earlywood and latewood indices of Scots pine and
676 Norway spruce on climatic factors in eastern Finland. *Ecol. Model.* 132, 259–273.
677

678 Miranda, I., & Pereira, H. (2002) Variation of pulpwood quality with provenances and site in
679 *Eucalyptus globus*. *Ann For. Sci.* 59, 283–291.
680

681 Newman, R.H. (1999) Estimation of the lateral dimensions of cellulose crystallites using ¹³C
682 NMR signal strengths. *Solid State Nuc. Mag. Res.* 15, 1-29.
683

684 Nielsen, L.R., & Kjær, E.D. (2008) Tracing timber from forest to consumer with DNA
685 markers. Danish Ministry of the Environment, Forest and Nature Agency. ISBN: 978-87-
686 7279-815-8 (accessed 30.10.2013) <http://curis.ku.dk/ws/files/8102944/TracingTimber.pdf>
687

688 Nimz, H.H., Robert, D., Faix, O., & Nemr, M. (1981) Carbon-13 NMR spectra of lignins:
689 structural differences between lignins of hardwoods, softwoods, grasses and compression
690 wood. *Holzforschung* 35, 16–26.
691

692 Nogueira, R.F., Tavares, M.I.B., & Nogueira, J. S. (2011) ¹³C NMR Molecular dynamic
693 investigation of tropical wood *Angelin Pedra* (*Hymenolobium paetrum*). *Mater.Sci.Appl.* 2,
694 453-457.
695

696 Okushita, K., Komatsu, T., Chikayama, E., & Kikuchi, J. (2012) Statistical approach for
697 solid-state NMR spectra of cellulose derived from a series of variable parameters. *Polymer J.*
698 44, 895–900.
699

700 Park, Y.I., & Spicker, H. (2005) Variation in the tree-ring structure of Norway spruce (*Picea*
701 *abies*) under contrasting climates. *Dendrochronologia* 23, 93–104.
702

703 Park, S., Baker, J.O., Himmel, M.E., Parilla, P.A., & Johnson, D.K. (2010) Cellulose
704 crystallinity index: measurement techniques and their impact on interpreting cellulase
705 performance. *Biotech. Biofuels* 3, 1-10.
706

707 Popescu, C.M., Larsson, P.T., & Vasile, C. (2011) Carbon-13 CP/MAS solid state NMR and
708 X-ray diffraction spectroscopy studies on lime wood decayed by *Chaetomium globosum*.
709 *Carbohydrate Polymers* 83(2), 808-812.
710

711 Preston, C.M., Trofymow, J.A., Niu, J., & Fyfe, C.A. (1998) ¹³CPMAS-NMR spectroscopy
712 and chemical analysis of coarse woody debris in coastal forests of Vancouver Island. *Forest*
713 *Ecology and Management* 111, 51–68.

714
715 Ritota, M., Casciani, L., Han, B.Z., Cozzolino, S., Leita, L., Sequi, P., & Valentini, M. (2012)
716 Traceability of Italian garlic (*Allium sativum* L.) by means of HRMAS-NMR spectroscopy
717 and multivariate data analysis, *Food Chemistry* 135(2), 684-693.

718
719 Ritota, M., Casciani, L., Failla, S., & Valentini, M. (2012) HRMAS-NMR spectroscopy and
720 multivariate analysis meat characterization, *Meat Science* 92(4), 754-761.

721
722 Sacchi, R., & Paolillo, L. (2007) NMR for Food Quality and Traceability, in L.M.L. Nollet &
723 F. Toldrá (Eds.) *Advances in Food Diagnostics* (pp. 101-117). Ames, Iowa, Blackwell
724 Publishing.

725
726 Samuel, R., Pu, Y., Faston, M., & Ragauskas, A.J. (2010) Solid-state NMR characterization
727 of switchgrass cellulose after dilute acid pretreatment. *Biofuels* 1(1), 85-90.

728
729 Sandak, A., Sandak, J., & Negri, M. (2010) Potential of mid and near infrared spectroscopy
730 for geographical origin recognition of forest based biomasses. III International Symposium on
731 Energy from Biomass and Waste, Venice, Italy, CISA Publisher.

732
733 Sandak, A., Sandak, J., & Negri, M. (2011) Relationship between near-infrared (NIR) spectra
734 and the geographical provenance of timber, *Wood Science and Technology* 45(1), 35–48.

735
736 Sivonen, H., Maunu, S.L., Sundholm, F., Jamsa, S., & Viitaniemi, P. (2002) Magnetic
737 resonance studies of thermally modified wood. *Holzforschung* 56, 648–654.

738
739 Skråppa, T., Høyen, G., & Dietrichson, J. (1999) Relationship between wood density
740 components and juvenile height growth and growth rhythm trials for Norway spruce
741 provenances and families. *Silvae Genetica* 48(5), 235–239.

742
743 Smerink, R.J., Baldock, J.A., & Oades, J.M. (2002) Impact of remote protonation on ¹³C
744 CPMAS NMR quantitation of charred and uncharred wood. *Solid State Nucl. Magn. Res.* 22,
745 71-82.

746
747 Smith, R.H., Peloquin, R.L., & Passoff, P.C., (1969) Local and regional variation in the
748 monoterpenes of ponderosa pine wood oleoresin. Oxford: U.S.D.A Forest Serv Res Paper
749 PSW-56, 10pp.

750
751 Spicker, H. (2000) Growth of Norway spruce (*Picea abies* [L.] Karst.) under changing
752 environmental conditions in Europe. *EFI Proceedings* 33, 11–26.

753
754 Tahar, D., Tayeb, B., & Chaabane, C. (2007) Essential oil composition of *Pinus halepensis*
755 Mill. from three different regions in Algeria. *J Essent. Oil Res.* 19, 40-43.

756
757 Tappi standard (2006) T 222 om-06. Acid insoluble lignin in wood and pulp.

758
759 Tappi standard (2007) T 204 cm-07. Solvent extractives of wood and pulp.

760

761 Tappi standard (2007) T 212 om-07. One percent sodium hydroxide solubility of wood and
762 pulp.
763
764 Tappi standard (2008) T 207 cm-08. Water solubility of wood and pulp.
765
766 Tappi standard (2007) T 211 om-07. Ash in wood, pulp, paper and paperboard: combustion at
767 525 °C
768
769 Teeäär, R., Serimaa, R., & Paakkarl, T. (1987) Crystallinity of cellulose, as determined by
770 CP/MAS NMR and XRD methods. *Polymer Bulletin*. 17(3), 231-237.
771
772 Viel, S., Capitani, D., Proietti, N., Ziarelli, F., & Segre, A.L. (2004) NMR spectroscopy
773 applied to the Cultural Heritage: a preliminary study on ancient wood characterization. *Appl.*
774 *Phys. A: Mater. Sci. Process.* 79, 357-361.

Table 1. General characteristics of the provenance sites

Country of origin	Country code	Elevation (m.o.s.l.)	Geographical coordinates		Climatic condition		Silvicultural details
			latitude	longitude	Average temperature	Average precipitation	
Italy	I	1700-1800	46° 11'	11° 50'	+2.4°C	1260mm	natural stand
Finland	F	140	63° 22'	30° 42'	+2°C	650mm	artificial forest
Poland	P	600-810	50° 44'	16° 9'	+8.4°C	600mm	zone of industrial emissions

Table 2. Contents of chemical components extracted from Norway spruce samples of different provenances

Country code	Cellulose %	Lignin %	Holocellulose %	Hemicellulose %	Extractives %	Hot water soluble %	1% NaOH soluble %	Ash %
	(± 1.36)	(± 0.25)	(± 1.80)	(± 1.50)	(± 0.32)	(± 0.30)	(± 0.60)	(±0.26)
I	45,5	28,8	70,4	24,9	1,15	0,87	10,65	0,3
F	45,2	28,4	70,2	25	1,82	2,05	11,48	0,3
P	45,7	29,3	70,2	24,5	1,84	0,56	9,73	0,3

Table 3. Physical characteristic of spruce samples.

Sample code	Density (g/cm³)	Late wood (%)	Age of tree (yr)	Average ring width (mm)
I1	0,42	0,27	127	1,08
I2	0,43	0,30	137	0,97
I3	0,39	0,17	131	1,60
F1	0,50	0,36	147	0,95
F2	0,56	0,38	141	1,14
F3	0,51	0,36	144	0,91
P1	0,46	0,30	100	1,59
P2	0,47	0,20	83	2,86
P3	0,45	0,28	99	1,80



Table 4. ^{13}C CPMAS resonance assignments of wood and HDPE

Signal Number*	Chemical shift (ppm)	Polymer assignments	Chemical species or carbon atom**
1	172.0	Carbohydrate;	-COO-R, CH ₃ -COO-
2	152.6	Lignin;	S3 (e), S5 (e)
3	147.0	Lignin;	S3 (ne), S5 (ne), G1, G4
4	136.0	Lignin;	S1 (e), S4 (e), G1 (e)
5	134.3	Lignin;	S1 (ne), S4 (ne), G1 (e)
6	121.0	Lignin;	G6
7	114–106	Lignin;	G5, G6, S2, S6
8	104.8	Carbohydrates;	C1
9	88.7	Carbohydrates;	C4 crystalline cellulose
10	83.8	Carbohydrates;	C4 amorphous cellulose; lignin C β
11	74.8	Carbohydrates;	carbohydrates; C2,3,5; lignin C α
12	72.2	Carbohydrates;	C2,3,5
13	64.7	Carbohydrates;	C6
14	61.6	Lignin;	C γ , C6
15	55.7	Lignin;	OCH ₃
16	32.3	Polyethylene	CH ₂
17	21.0	Carbohydrates;	CH ₃ -COO-

* reported in Figure 3

** according to labelling of Figure 2

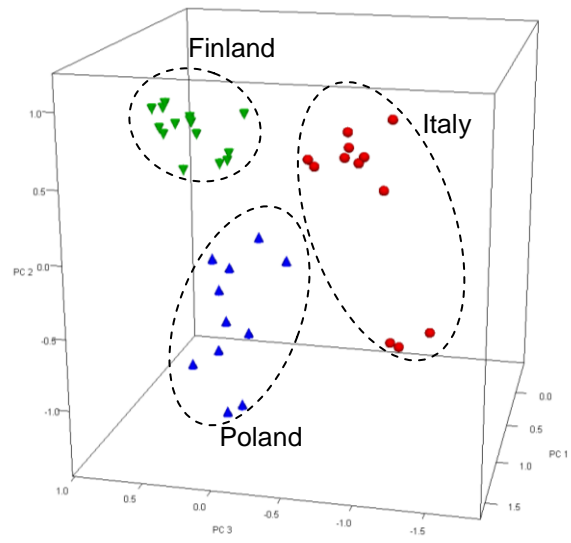


Figure 1. FT-IR-based discrimination of the spruce woods due to provenance

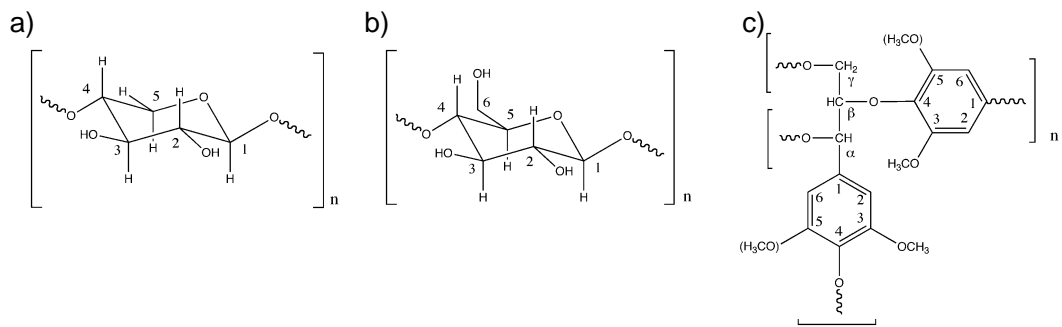


Figure 2. The chemical structures of the main wood components (according to Bardet et al. 2009): cellulose (a), hemicellulose (b) and lignin (c), and the numbering scheme corresponding to the resonance peaks summarized in Table 4

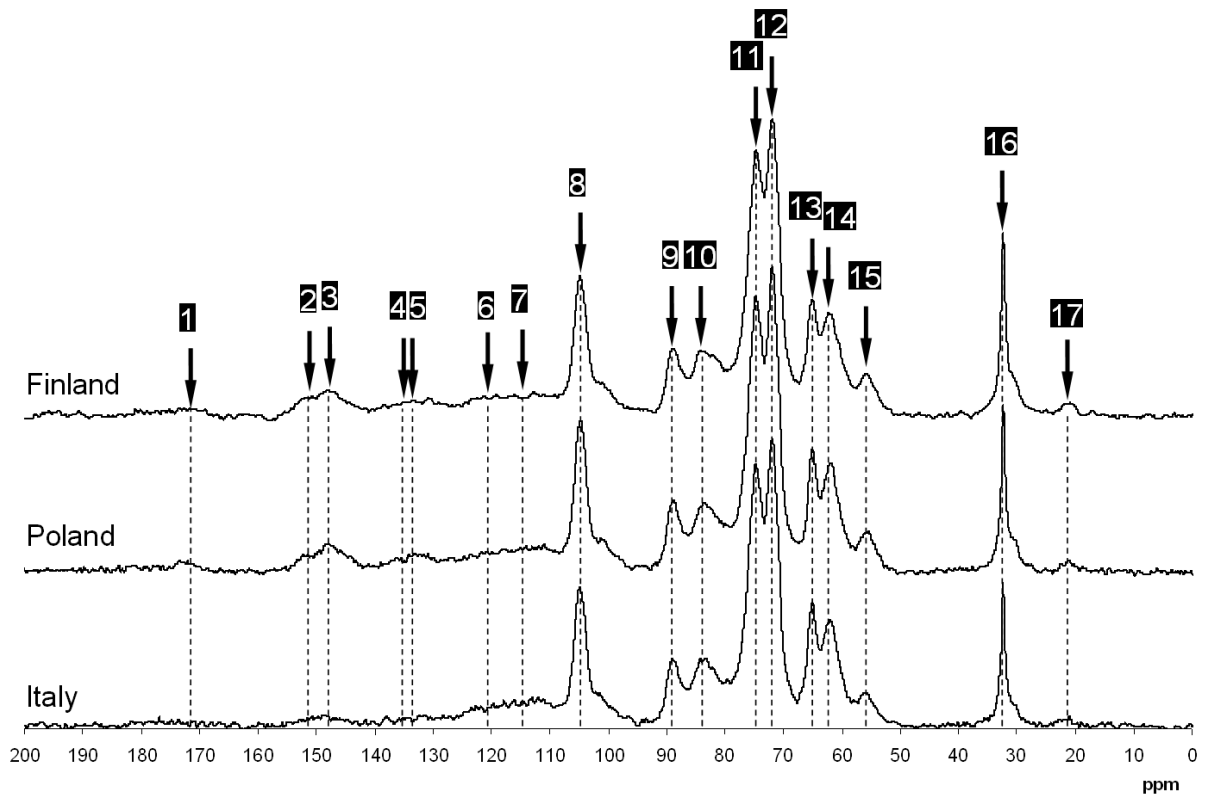


Figure 3 NMR spectra of spruce woods differing in provenance and the peaks assignments

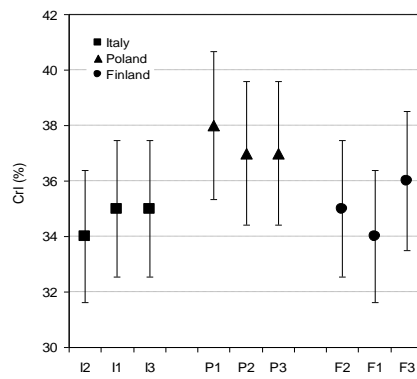


Figure 4. Cellulose crystalline index CrI computed from the NMR spectra of spruce from different provenance

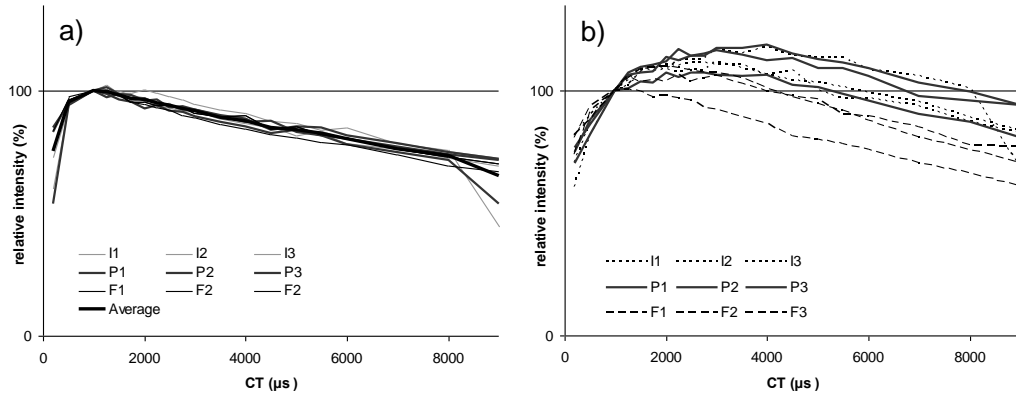


Figure 5. Normalized peak intensity vs ct of HDPE signal 16 (a) and wood signal 8 (b).

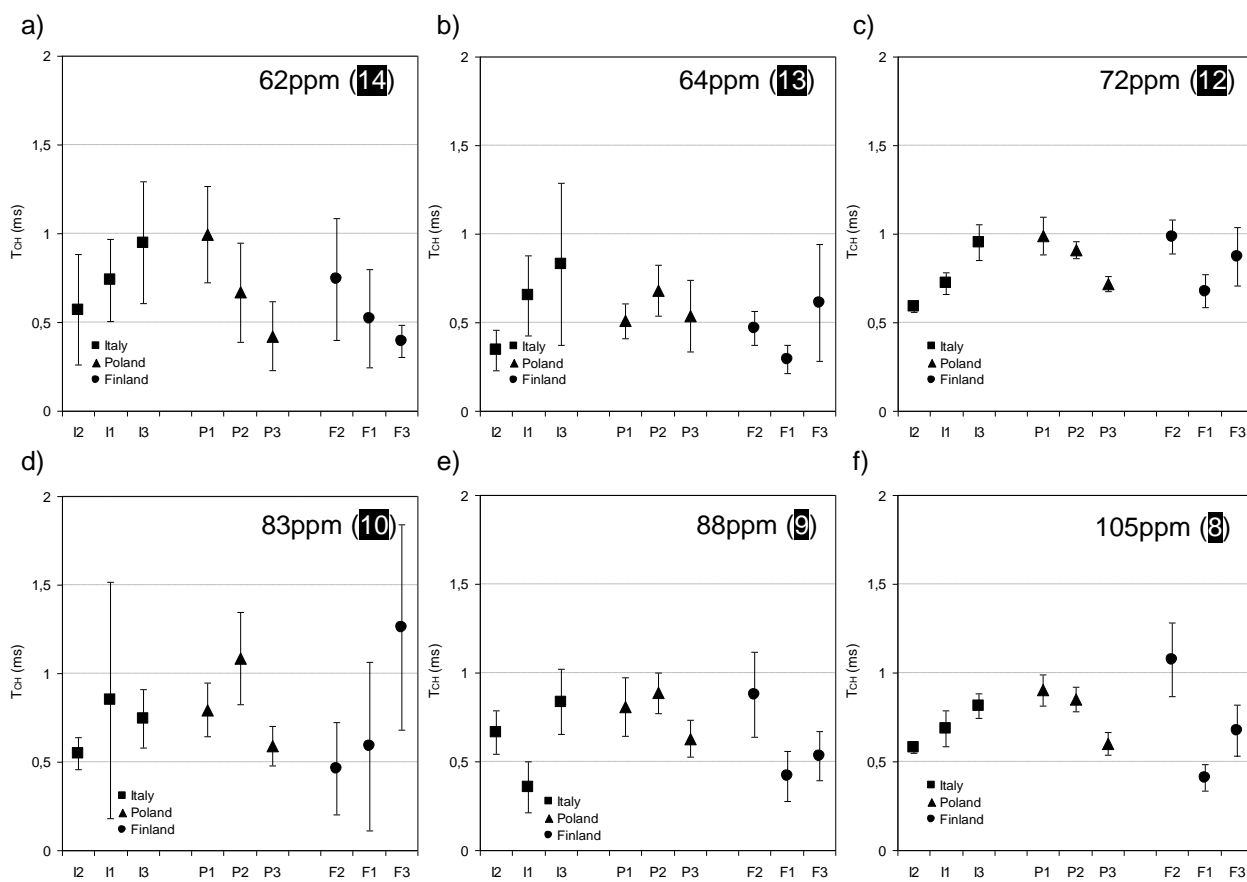


Figure 6. T_{CH} values obtained from the fitting of VCT curves of selected ^{13}C signals with Equation 1.

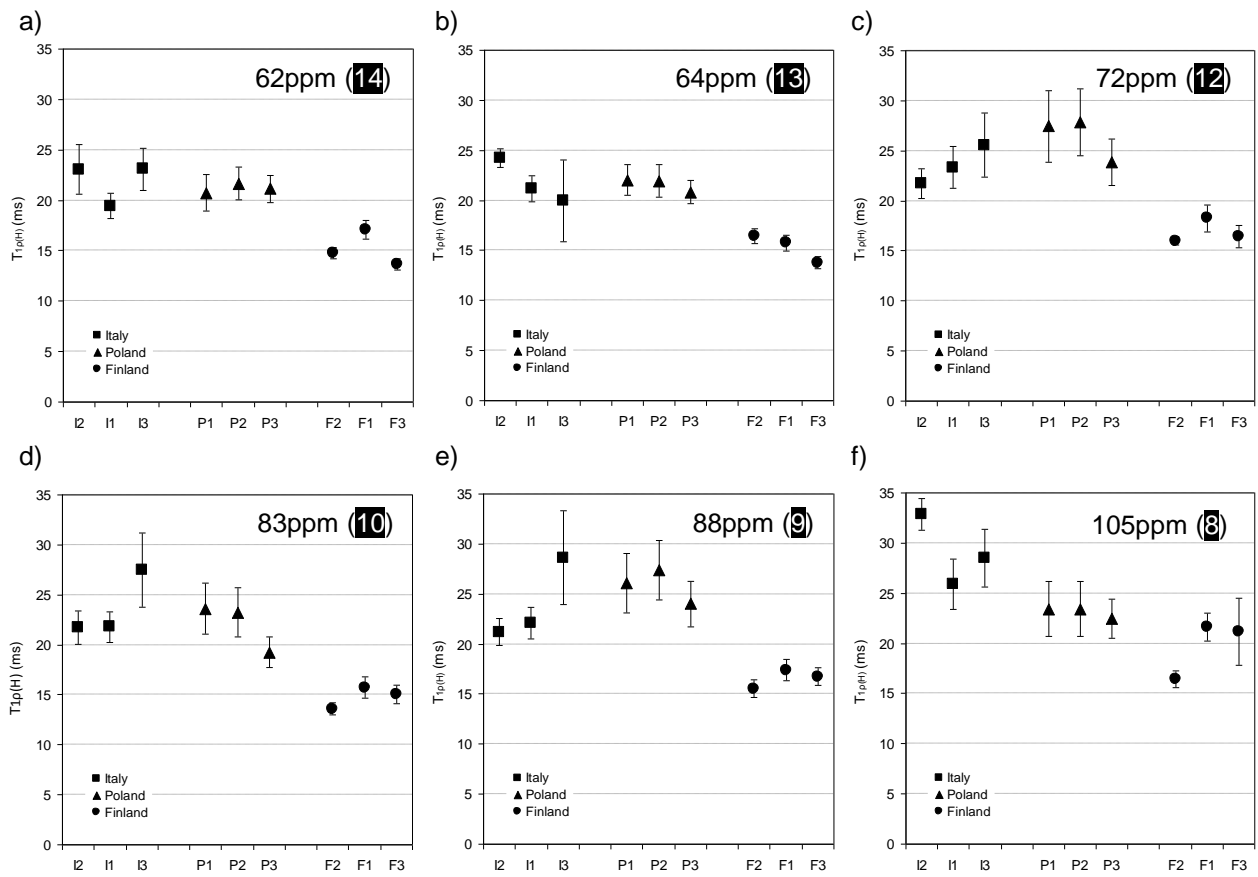


Figure 7. $T_{1\rho(H)}$ values obtained from fitting VCT curves of selected ^{13}C signals with Eq. 1

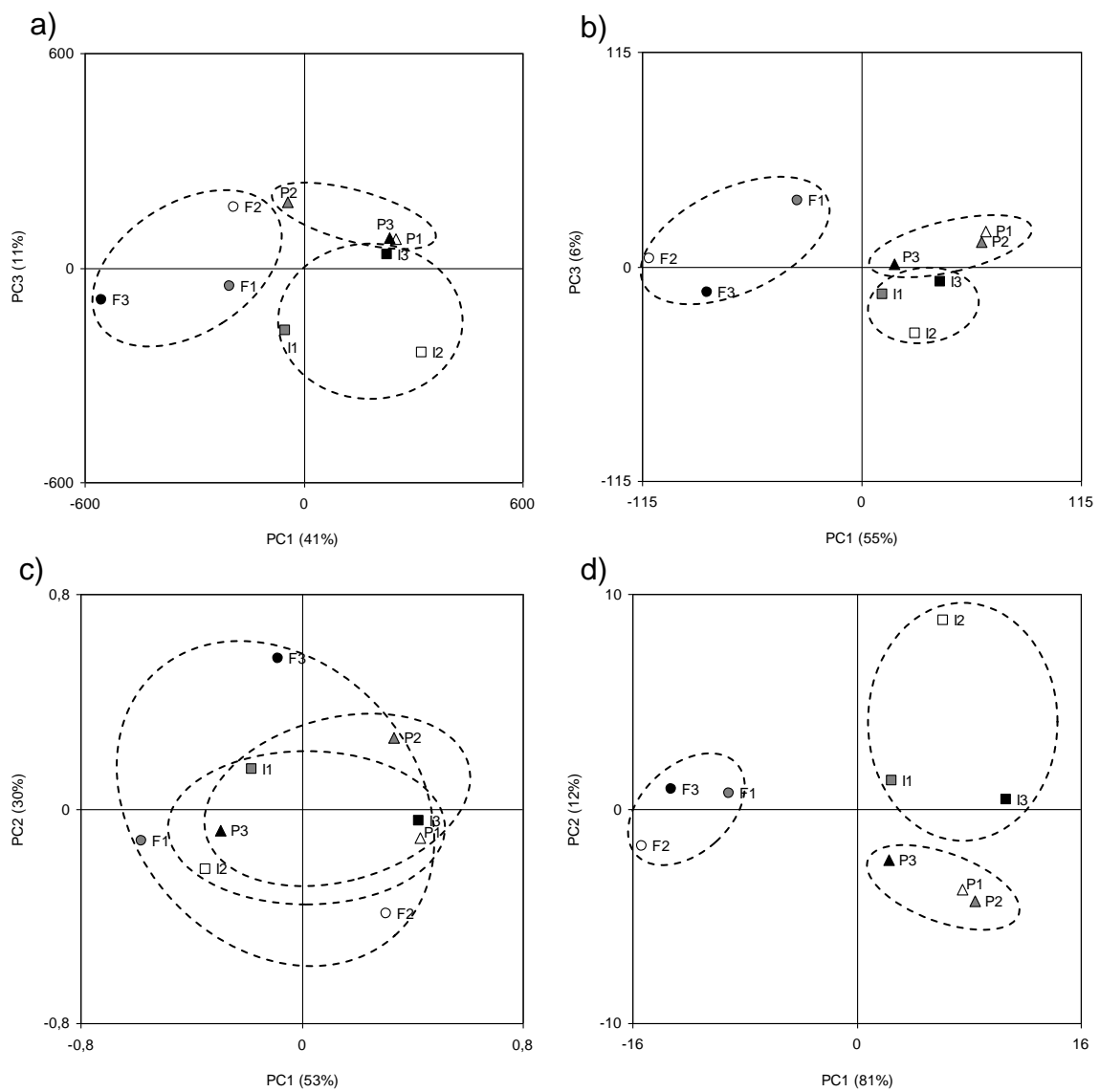


Figure 8. Principal Components Analysis of; all NMR spectra (a), dataset of all the VCT curves of selected peaks (b) and T_{CH} (c) and $T_{1\rho(H)}$ (d) computed from VCT curves